Intelligent Pavement for Traffic Flow Detection – Phase II

Final Report

Prepared by:

Xun Yu

Department of Mechanical and Industrial Engineering
University of Minnesota Duluth

Northland Advanced Transportation Systems Research Laboratories
University of Minnesota Duluth

CTS 12-30

Technical Report Documentation Page

1. Report No.	2.	3. Recipients Accession No.	
CTS 12-30			
4. Title and Subtitle		5. Report Date	
Intelligent Pavement for Traffic Flow Detection – Phase II		September 2012	
		6.	
7. Author(s)		8. Performing Organization Report No.	
Xun Yu			
9. Performing Organization Name and Address		10. Project/Task/Work Unit No.	
Department of Mechanical and Industrial Engineering University of Minnesota Duluth 1305 Ordean Court Duluth, MN 55812		CTS Project #2010002	
		11. Contract (C) or Grant (G) No.	
12. Sponsoring Organization Name and Address		13. Type of Report and Period Covered	
Intelligent Transportation Systems Institute Center for Transportation Studies University of Minnesota 200 Transportation and Safety Building 511 Washington Ave. SE Minneapolis, Minnesota 55455		Final Report	
		14. Sponsoring Agency Code	
15. Supplementary Notes			
http://www.its.umn.edu/Publications/ResearchReports/			

16. Abstract (Limit: 250 words)

This project is the extension of a Northland Advanced Transportation System Research Laboratory (NATSRL) FY09 project, titled as "Intelligent Pavement for Traffic Flow Detection", which aims to explore a new approach in detecting vehicles on a roadway by making a roadway section as a traffic flow detector. Sections of a given roadway are paved with carbon-nanotube (CNT) enhanced pavement; the piezoresitive property of carbon nanotubes enables the pavement to detect the traffic flow. Meanwhile, CNTs can also work as reinforcement elements to improve the strength and toughness of the concrete pavement. The proposed sensor is expected to have a long service life with little maintenance and wide-area detection capability. In the FY09 project, lab tests demonstrated that CNT based cement composite can detect the mechanical stress levels for both static and dynamic loads. In the FY10 project, the research was extended to cement mortar, which has much higher mechanical strength and more useful in real applications. The effects of water level and CNT doping levels on the piezoresistivity of the composites were also studied. Preliminary road tests were performed for the evaluation of this new traffic sensor.

17. Document Analysis/Descriptors		18. Availability Statement	
Traffic detector, Vehicle detectors, Carbon nanotube, Composite pavements, Piezoresistive, Resistivity method		No restrictions. Document available from: National Technical Information Services, Alexandria, Virginia 22312	
19. Security Class (this report)	20. Security Class (this page)	21. No. of Pages	22. Price
Unclassified	Unclassified	33	

Intelligent Pavement for Traffic Flow Detection – Phase II

Final Report

Prepared by:

Xun Yu

Department of Mechanical and Industrial Engineering
University of Minnesota Duluth

Northland Advanced Transportation Systems Research Laboratories
University of Minnesota Duluth

September 2012

Published by:

Intelligent Transportation Systems Institute
Center for Transportation Studies
University of Minnesota
200 Transportation and Safety Building
511 Washington Ave. S.E.
Minneapolis, Minnesota 55455

Acknowledgments

The authors wish to acknowledge those who made this research possible. The study was funded by the Intelligent Transportation Systems (ITS) Institute and Northland Advanced Transportation System Research Laboratory (NATSRL). The ITS Institute is a program of the University of Minnesota's Center for Transportation Studies (CTS). Financial support was provided by the United States Department of Transportation's Research and Innovative Technologies Administration (RITA). NATSRL is a transportation research program at the University of Minnesota Duluth and its partners include the Minnesota Department of Transportation, the ITS Institute, St. Louis County and the City of Duluth.

We thank Dr. Eil Kwon, director of NATSRL, for many productive discussions.

We also thank the hard work of Dr. Baoguo Han, the research associate who made significant contributions to this project.

Table of Contents

List of Figures

List of Tables

Executive Summary

This project explored a new approach in detecting vehicles on a roadway by making a roadway section a traffic flow detector. Carbon-nanotube (CNT)/cement composites were investigated for this purpose. The piezoresitive property of carbon nanotubes enables the composite to detect traffic flow. Meanwhile, CNTs can also work as reinforcement elements to improve the strength and toughness of concrete pavement.

Piezoresistive CNT/cement composites (cement mortar) were developed and tested in this study. Experimental results show that the electrical resistance of the composite changed proportionally to the compressive stress levels. The piezoresistive responses of the composite with water level and CNT doping levels were also studied. The composites showed non-linear responses to both water levels and CNT doping levels. The experimental results, including the lab tests and preliminary road tests, demonstrated the potential of using the CNT/cement composite as a traffic flow detector.

In contrast to current traffic flow detection technologies that require separate devices to be installed either in the pavement or over the road, the proposed sensing approach enables the pavement itself to detect traffic flow parameters. Therefore, the proposed sensor is expected to have a long service life with little maintenance and wide-area detection capability.

Chapter 1. Introduction

1.1 Review of Traffic Flow Sensors

Traffic flow sensors are an integral part of modern intelligent transportation systems (ITS). Sensors provide real-time input data in support of a variety of ITS services and strategies, such as freeway ramp metering, traffic signal control, driver information and guidance. Therefore, the success of ITS depends to a large extent on the accuracy and reliability of traffic flow sensors.

A large number of researchers have investigated different kinds of traffic sensing technologies. These sensors can be categorized into two major classes [1-3]:

- **In-roadway (intrusive) sensor**: it is embedded in the pavement such as inductive loop detectors and magnetometers.
- **Over-roadway (non-intrusive) sensor**: this kind of sensor is mounted over the roadway such as microwave radar sensors, ultrasonic sensors, laser radar sensors, infrared sensors, and video image processors.

Among these various sensors, inductive loop detectors are the predominant traffic flow sensors, due to their mature technology, insensitive to weather conditions, and relative low costs. The configuration of an inductive loop detector is shown in Figure 1 [3], which typically consists of a coil that is embedded in the road, a pull box, a lead-in cable, and a controller. As the vehicle passes over the coil, the inductance of the coil will reduce, which will change the oscillation frequency of an oscillator.

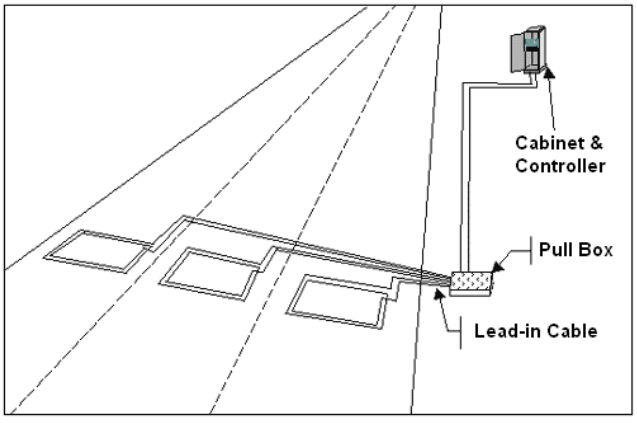

Figure 1. Configuration of an inductive loop detector [3]

Inductive loop detector can accurately measure occupancy, vehicle speed, and gaps. However, there are several limitations with inductive loop detectors:

1. Installation of inductive loops requires pavement cut (the typical size of a loop is 6 ft x 6 ft).
2. Installation and maintenance require lane closure, which could bring severe traffic congestion and high maintenance cost.
3. Wire coil suffers from the stresses of traffic and temperature.

4. If not properly installed, the inductive loop will decrease the pavement life.

The above issues with inductive loops and recent advances in computing and communication technologies have led to the development of non-intrusive detection technologies, such as microwave radars, infrared sensors, and video image processors. However, these non-intrusive sensors face limitations of high sensor costs, high maintenance cost, and poor performance in inclement weather conditions (rain, snow, and fog). Many of them also need additional mounting structures and time-consuming calibration. These limitations make the intrusive sensors (mainly inductive loops) still primary traffic detection systems in the field. The lack of low cost, low maintenance, long service, and reliable traffic detectors motivates this proposed research.

1.2 Review of CNT and CNT-Based Composites

In this project, we propose the investigation of carbon nanotube (CNT)/cement composites for traffic flow measurement by detecting the change of electrical resistance of the composite when subject to the stress of a vehicle. Being an integral part of the pavement with strong mechanical strength, the proposed traffic sensor will provide several advantages over the inductive loop detectors, such as easy installation and maintenance, long service life and little maintenance, wide detection area, and potential applications for structural health monitoring.

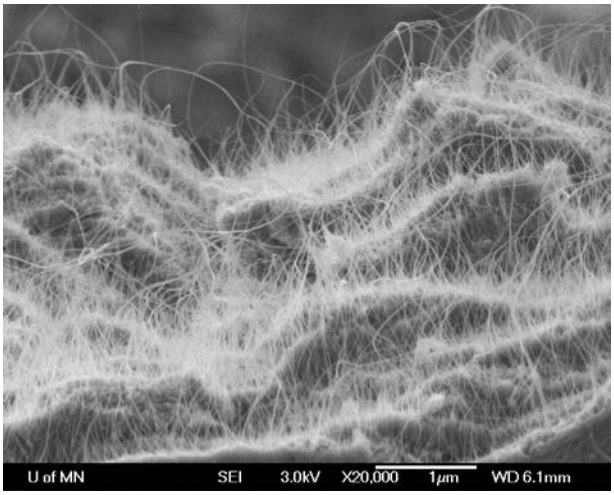

Figure 2. A SEM (scanning electron microscope) picture of CNTs

Carbon nanotubes (CNTs) are seamless tubular structures rolled up forming a one-atom sheet of graphite, with diameter in the order of a nanometer (10^{-9}m). The nanotubes may consist of one shell of carbons (single-walled carbon nanotubes (SWNTs)), or up to tens of concentric shells of carbons (multi-walled carbon nanotubes (MWNTs)). The diameters of CNTs are in the range of 1~20 nm, and the lengths are in the range of 0.2~5 μm.

Since the discovery of CNTs by S. Iijima in 1991 [4], carbon nanotubes have been widely used for a variety of applications due to their excellent physical properties: high strength (the Young's modulus of individual CNTs is about 1.8 TPa) [5], metallic or semi-conductive electrical properties depending on their roll up charity [5]; and high aspect ratio (>500). The extremely high aspect ratio of CNTs makes them easy to form a conductive and reinforcement network

with doping level as low as 0.1% wt of CNTs [6-8]. Carbon nanotubes also have interesting electromechanical properties. When subject to stress/strain, the electrical properties of CNTs will change with the level of stress/strain, expressing a linear and reversible piezoresistive response [9-12]. Most of those prior works were performed with individual nanotubes or nanotube membranes. Recently, CNT/polymer composites have also been investigated for strain/stress sensing [13]; their results also show linear electrical resistance changes with respect to the strain/stress and the sensitivity is 3.5 times of regular stain gage. These previous works show that CNT based composite could be a promising stress/strain sensor. However, no previous study has been performed on the piezoresistive responses of the CNT/cement composites. Since the properties of cement are much different from polymers, it would be very interesting to investigate the electromechanical property of the CNT/cement composite, and how the interface between CNTs and cement will influence the electromechanical property of the composite.

On the other hand, with the advances of CNT synthesis techniques, the price of CNTs has decreased dramatically in recent years. For example, MWNT can be purchased at $0.2/g (TimesNano, China). The decreasing price and the ultra low needed doping level of CNTs enable them possible to be used in large structures, e.g., concrete pavements, which had not been investigated by previous studies.

A literature survey reveals very few previous research efforts on the CNT/cement composites. Li *et. al.* studied the mechanical properties of CNT/cement composites [14]. They found that the compressive strength and flexural strength of the 0.5% CNT cement composites were increased by 19% and 25% respectively, compared to the un-reinforced cement. However, they did not study the piezoresistive properties of CNT/cement composites. Another research group in Canada conducted a similar mechanical reinforcement study but not the piezoresistive behavior of the composites [20].

It should be noted that another class of carbon material – carbon fibers (CFs), have been extensively studied as reinforce elements in cement concrete. CFs are different from CNTs with much larger diameters (1~15 μm), smaller Young's modulus (~560 MPa) and aspect ratio [15]. The piezoresistivity and piezoelectric properties of CF/cement have also been investigated by Chung *et. al.* [16-18] and Sun *et. al.*[19]. However, it was found that the piezoresistivity and piezoelectric of the CFs would be *irreversible* due to the fiber breakage when the strain was larger than 0.2% [16]. Therefore, CF/cement composite is not appropriate as a strain/stress sensor to detect heavy stresses of traffic flows. On the contrary, Tombler *et. al.* found that the piezoresistive characteristics of CNTs were highly reversible even for a huge strain of 3.4% [9]. This indicates CNT/cement could be a promising distributed stain/stress sensor for traffic flow detection.

1.3 Summary of FY 09 Results

In FY09 project, several fabrication methods have been explored to fabricate CNT/cement composites that show very promising piezoresistive properties. In short, in order to fully disperse CNTs into cement matrix, CNTs were either treated with acid or dispersed with chemical surfactants to make stable dispersion in water. The CNT/cement composites were then tested in lab with compressive loads while measuring its electrical resistance changes. Figure 3 shows the typical electrical response of the composite to different types of compressive loads.

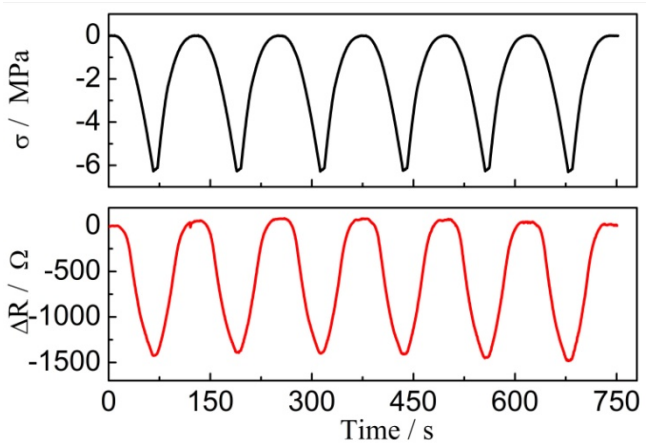

a) Under repeated compressive loading with amplitude of 6MPa

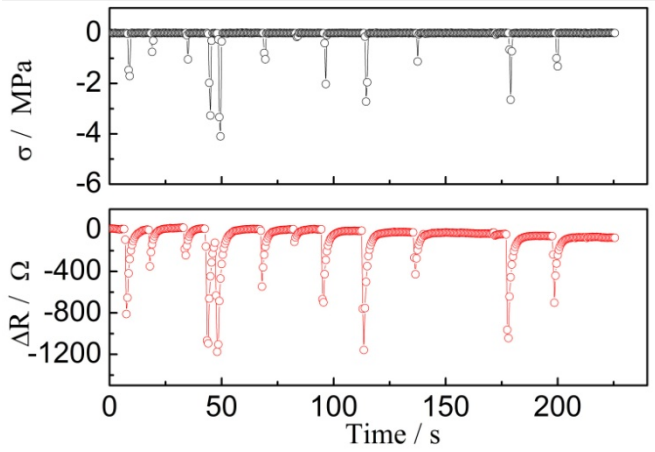

b) Under impulsive loading

Figure 3. Relationships between compressive stress and electrical resistance of the self-sensing CNT/cement composite

Chapter 2. Piezoresitve Response of CNT/Cement Mortar

In FY09 project, the composites were CNT/cement paste, i.e., they did not contain sands or aggregates. Cement paste has low compressive strength so it is not very useful in real structures. In this FY10 project, we extend the study to cement mortar, which has sands in the composite. The cement mortar has much higher mechanical strength and is much more commonly used in civil structures.

In this study, the cement used is Portland cement (ASTM Type I) provided by Holcim Inc., USA. The MWNTs used are carboxyl MWNTs provided by Timesnano, Chengdu Organic Chemicals Co. Ltd. of Chinese Academy of Sciences, China. Their properties are given in Table 1. Figure 4 shows a scanning electron microscope (SEM) picture of the received MWNTs. The surfactant used for dispersing the MWNTs is sodium dodecylbenzene sulfonate (NaDDBS), it is provided by Sigma-Aldrich Co., USA. Tributyl phosphate (Sigma-Aldrich Co., USA) is used as defoamer to decrease the air bubble in MWNTs filled cement-based composites caused by use of NaDDBS.

Table 1. Properties of carboxyl multi-wall carbon nanotubes

Parameters	Values
Outside diameter	<8nm
Inside diameter	2~5nm
-COOH content	3.86 wt.%
Length	10~30μm
Purity	>95%
Ash	<1.5 wt.%
Special surface area	>500 m2/g
Electrical conductivity	>102 s/cm
Density	~2.1 g/cm3

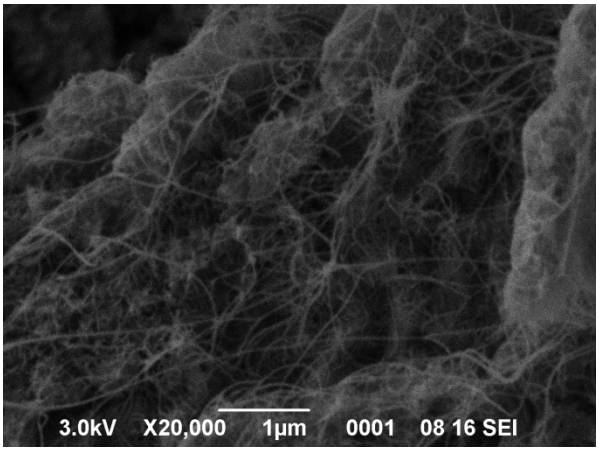

Figure 4. SEM picture of as-received MWNTs

The 1.4×10-2mol/L of the critical micelle concentrations in water of NaDDBS was taken as the input surfactant concentration. The surfactant was firstly mixed with water (the water/cement ratio is 0.46:1) using a magnetism stirrer (PC-210, Corning Inc., USA) for 3 min. Next, MWNTs were added into this aqueous solution and sonicated with an ultrasonicator (2510, Branson Ultrasonic Co., USA) for 2h to make a uniformly dispersed suspension. Then, a mortar mixer was used to mix this suspension, cement and sand (the ratio of sand to cement is 1.5:1) for about 3 min. Finally, a defoamer in the amount of 0.25 vol. % was added into the mixture and mixed for another 3 min. The addition rates of MWNTs are 0.08% and 0.4% by weight for MWNTs filled cement mortar.

After casting the mixes into oiled molds (5.08×5.08×5.08cm) and embedding two stainless steel gauzes (with opening of 1.25×1.25cm) as two electrodes with 1cm apart, an electric vibrator was used to ensure good compaction. The specimens were then surface-smoothed, and covered with plastic films. All specimens were demolded 24h after casing. Thereafter, they were cured under the standard condition at a temperature of 20°C and a relative humidity of 100% for 28 days. All specimens were dried at a temperature of 50°C for five days before testing.

Electrical resistance measurements were made by a two-electrode method using a digital multimeter (Keithley 2100, Keithley Instruments Inc., USA) [18]. Compressive loads were applied using a material testing machine (ATS 900, Applied Test Systems, Inc., USA). All of the measurements interfaced with a PC were automatically recorded. All the experiments were carried out at room temperature. At least three specimens of each composite were tested.

The variation in electrical resistance of cement mortar with 0.4 wt.% of MWNTs under repeated compressive loading and impulsive loading is illustrated in Figure 5. As shown in Figure5 a), the relationships between the change in electrical resistance of the composite and the compressive stress are similar to that of MWNTs filled cement paste. The change in electrical resistance decreases about 400Ω and 700Ω as the compressive stress is 6MPa and 10MPa respectively, which indicate a little weaker piezoresistive response than that of cement paste. In addition, Figure5 b) shows that there is a good correlated relationship between the electrical resistance and the impulsive loading.

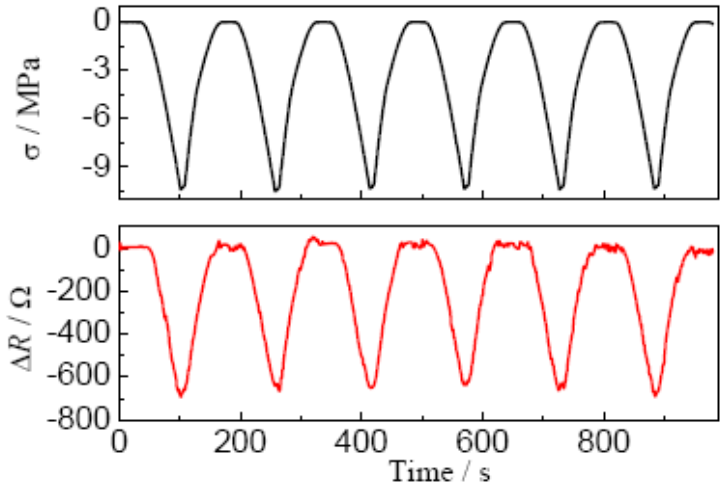

a) Under repeated compressive loading with amplitude of 10MPa

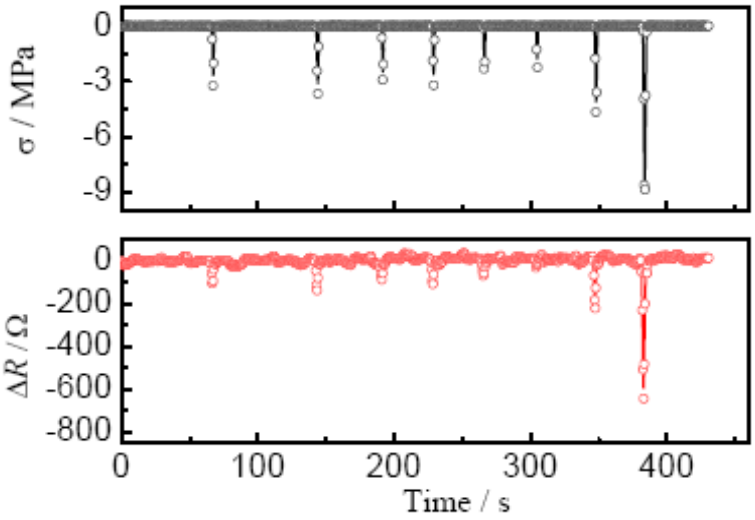

b) Under impulsive loading

Figure 5. Piezoresistivity of cement mortar with 0.4 wt.% of MWNTs

Figure 6 shows that the response of electrical resistance of cement mortar with 0.08 wt.% of MWNTs on compressive stress under repeated compressive loading and impulsive loading. Comparing Figs. 5 and 6 carefully, we find that the change trend of electrical resistance of the composites with 0.08 wt.% of MWNTs is similar to that of the composites with 0.4 wt.% of MWNTs, but their change only reach about 200Ω and 350Ω maximum respectively for compressive loading of 6MPa and 10MPa. The repeatability of the variation of electrical resistance in each cycle under repeated loading is also worse than that of cement mortar with 0.4 wt.% of MWNTs. In addition, as can be seen from Figure 6 b), the composite shows weaker piezoresistive responses to impulsive loads.

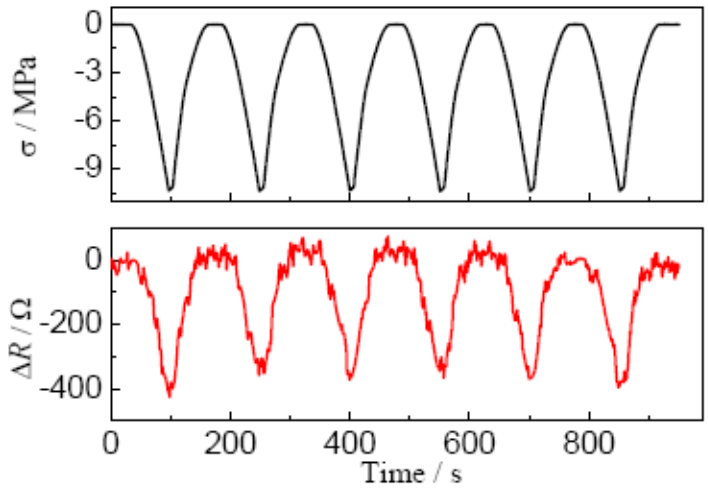

a) Under repeated compressive loading
with amplitude of 10MPa

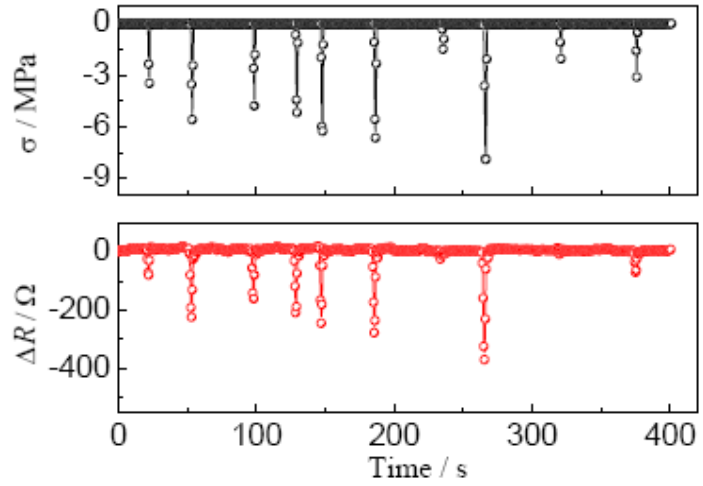

b) Under impulsive loading

Figure 6. Piezoresistivity of cement mortar with 0.08 wt.% of MWNTs

Chapter 3. Effects of Water Level and CNT Doping Level on the Piezoreistive Property of CNT/Cement Composite

3.1 Effect of Water Level on the Piezoresistivity of CNT/Cement Composite

To be used for real application, the self-sensing composites will experience different environmental conditions. One very important parameter is water/humidity inside the concrete. In this study, the effect of water level on the performance of CNT/cement composite is investigated.

The water content and the piezoresistivity of samples were measured over a drying period of time ranging from 2 hours to 35 days. The water content measurement was measured using an electronic scale (PG5002-S, Mettler Toledo Inc., USA). The water content C_w can be denoted by

$$C_w = \frac{W_s^t - W_s^0}{W_s^0} \times 100\% \qquad (1)$$

where W_s^t is the mass of samples when the time is t during drying, W_s^0 is the constant mass of samples when the drying time excesses 28 days under the condition at a temperature of 20°C and a relative humidity of 30%.

Figure 7 shows the piezoresistive responses of samples with different water contents under repeated compressive loading with amplitude of 6MPa. The piezorsistive sensitivities k ($k = \left|\frac{\Delta R}{\Delta \sigma}\right| \times 100\%$) are fitted using a linear regression. As can be seen in this figure, the electrical resistance of MWNTs/cement composites decreases linearly and reversibly upon loading and increases linearly and reversibly upon unloading in every cycle under compressive loading, expressing regular and stable piezoresitive responses, while composites with different water contents yield different levels of resistance changes.

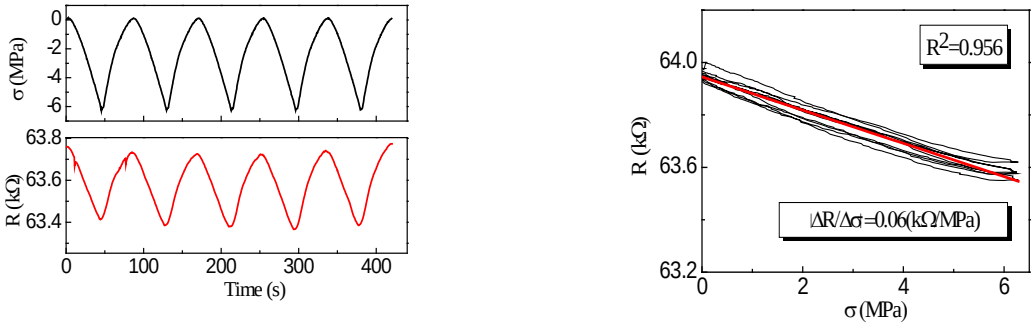

a) With 9.9% of water content

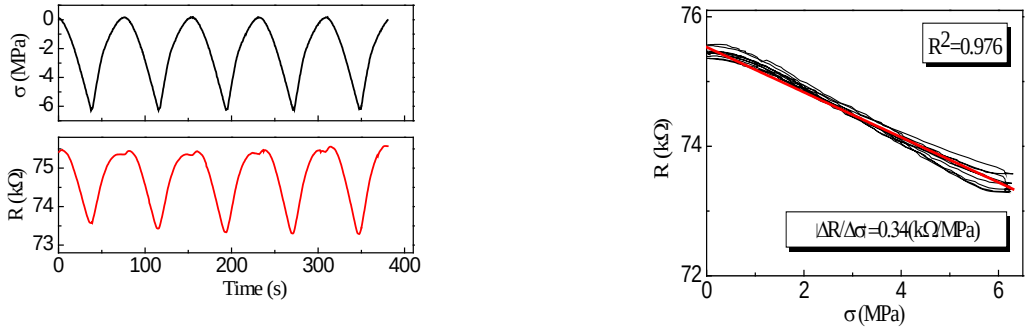

b) With 7.6% of water content

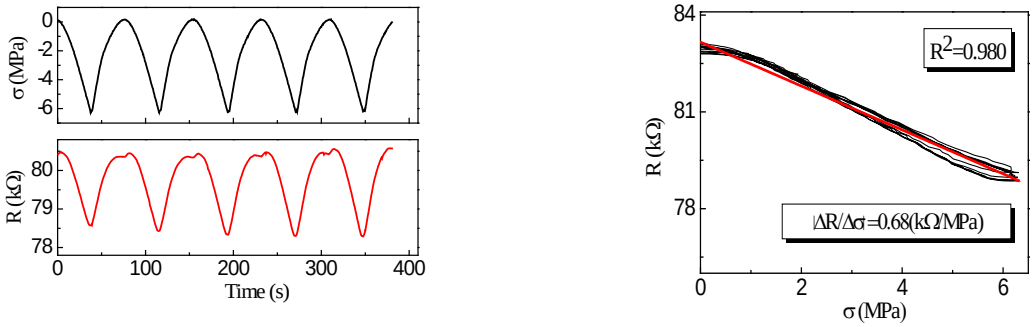

c) With 5.7% of water content

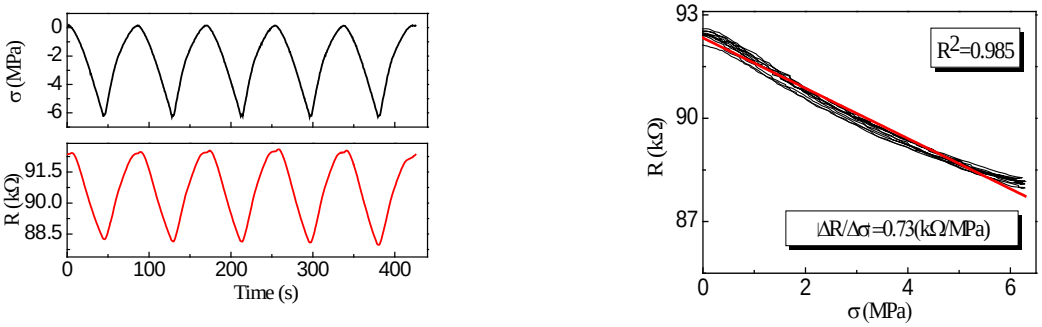

d) With 3.3% of water content

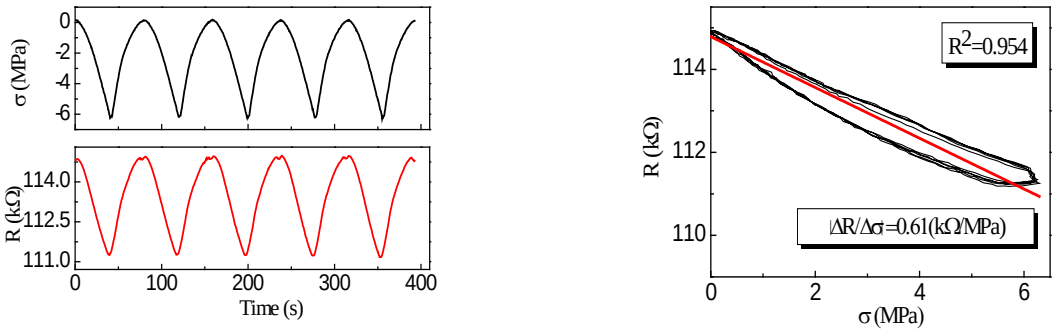

e) With 1.3% of water content

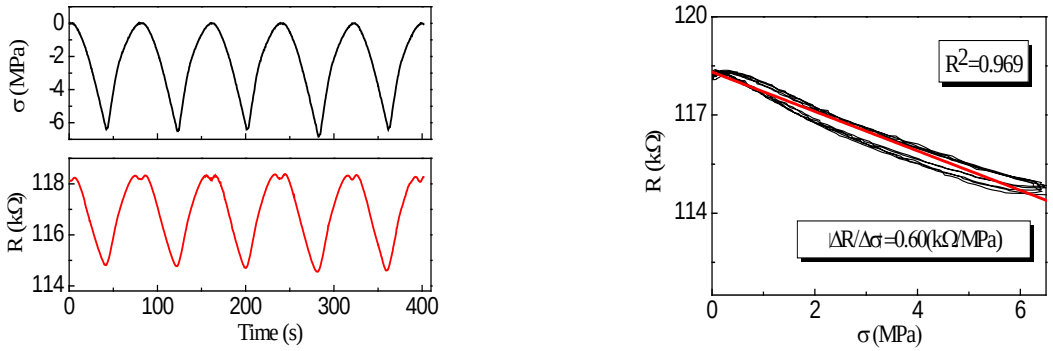

f) With 0.1% of water content

Figure 7. Piezoresistivity of MWNTs/cement composites with different water contents

The electrical resistance of CNTs/cement composites comes from two sources, i.e., the intrinsic resistance of nanotubes and the contact resistance (i.e. the resistance of the matrix connecting the crossing nanotubes and through which electrical tunneling occurs) as shown in Figure8. The electric conductivity of individual CNTs is in the order of 10^4~10^7s/m. But the contact resistance at nanotube junctions is rather complicated and depends on physical characteristics of nanotubes, tunneling gap at contact points and conductive properties of matrix filling the tunneling gap. The electrical resistance of MWNTs/cement composites can be changed when they are deformed under applied loading. Several factors may contribute to the electrical resistance change. First, when MWNTs/cement composites are deformed under external loading, the nanotube length and diameter will alter, resulting in the change of nanotube intrinsic resistance, and hence, the electrical resistance of the nanotube network. However, this resistance change is expected to be negligible because of the extremely small elastic deformation in nanotubes. The second and more important factor contributing to the resistance change of the composites is the contact resistance. Under applied load, the thickness of the insulating matrix between adjacent nanotubes may be changed considerably. The compressive loading gives rise to the decrease of the gap at the contact area where electrical tunneling takes place and thus decreases the contact resistance.

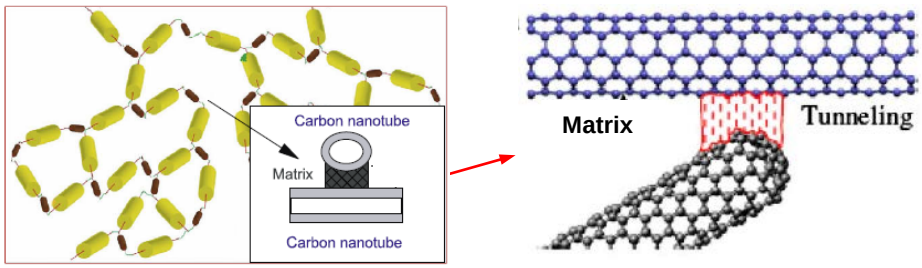

Figure 8. A schematic diagram of conductive network in CNTs/cement composites

Figure9 shows the initial electrical resistances R_0, the maximum change amplitudes f ($f = \left| \frac{R_{6MPa} - R_0}{R_0} \times 100\% \right|$, where R_{6MPa} is the electrical resistance of samples when the compressive stress is 6MPa) of electrical resistance and piezoresistive sensitivities of samples with different water contents. It can be found from Figure9 that the maximum change amplitudes of electrical resistance and piezoresistive sensitivity of samples with 3.3% of water content are the highest among composites with different water contents. The above results indicate that the piezoresistive sensitivities of the composites firstly increase and then decrease with the increase of water content in the composites.

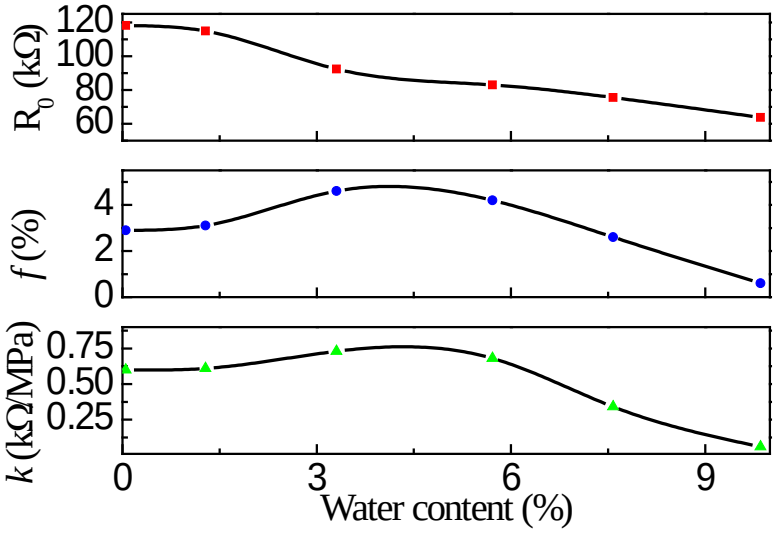

Figure 9. Comparison of electrical resistances, maximum change amplitudes of electrical resistance and piezoresistive sensitivities of MWNTs/cement composites with different water contents

It is interesting to note that the piezoresistive sensitivity of the composites does not linearly increase with water content, but the electrical conductivity of the composites as shown in Figure9 increases with water content. This phenomenon can be explained below. Two factors would contribute to the effect of water content on the sensitivity of piezoresistive response. One is the electrical conductivity of matrix, and the other is the field emission effect on the nanotube tip. The electrical conductivity of matrix and the field emission effect on the nanotube tip can be enhanced by the adsorption of water molecules. When the water content is 0.1%, the electrical conductivity of matrix filling the tunneling gap is low (i.e. the contact resistance is high) and the field emission effect on the nanotube tip is weak. The conductive path is thus hard to form, even when an external force is applied to the composites. As a result, the composites possess high electrical resistance and low sensitivity to stress. With the increase of the water content to 3.3%, the electrical conductivity of matrix filling the tunneling gap increases (i.e. the contact resistance decreases) and the field emission effect on the nanotube tip is enhanced. This increases the electrical conductivity of composites. Furthermore, when the composites deform under compressive loading, the tunneling barrier of electrons will decrease and the field emission induced tunneling can easily occur in the composites. These cause the composites present lower

electrical resistance and higher piezoresistive sensitivity. With the continuous increase of water content to a higher level such as 9.9%, the electrical conductivity of matrix filling the tunneling gap further increases (i.e. the contact resistance further decreases) and the field emission effect on the nanotube tip is enhanced, and then the conductive network stabilizes and becomes hardly to change under loading. As a result, a too higher water content will induce a much lower electrical resistance and a lower sensitivity to stress. Therefore, the sensitivity of piezoresistive response of MWNTs/cement composites is highly influenced by the water content in the composites, and it firstly increases then decreases with the increase of water content in the composites.

3.2 Effect of CNT Doping Level on the Piezoresitvity of CNT/Cement Composite

CNT concentration level is one important parameters for the mix design of piezoresistive CNT/cement composites. The effects of CNT concentration level on the piezoresistivity of these composites deserve extensive investigation for further optimizing the sensing property of the composites. In this project, the CNT/cement composites with different MWNT concentration levels are fabricated. By comparing the responses of electrical resistance of these CNT/cement composites to compressive stress, the effects of the CNT concentration level on the piezoresistive sensitivity are investigated.

Table 2 describes the mix proportions of the five types of CNT/cement composites in this study.

Table 2. Mix proportions of five types of CNT/cement composites

Sample	CNT/cement ratio	Water/cement ratio	Surfactant		Defoamer vol. %
			Type	Concentration	
#1	0.05%	0.45	NaDDBS	1.4×10^{-2}mol/L	0.25
#2	0.1%	0.45	NaDDBS	1.4×10^{-2}mol/L	0.25
#3	1%	0.45	NaDDBS	1.4×10^{-2}mol/L	0.25

Figure 10 shows the piezoresistive responses under repeated compressive loading with amplitude of 6MPa for samples #1, #2 and #3 listed in Table 2. The change in electrical resistance ΔR is calculated from $R - R_0$, where R_0 is the initial electrical resistance of samples without compressive loading. However, it should be noted that the electrical resistance of CNT/cement composites without compressive loading is time-variant due to the existence of the polarization effect. Therefore, the initial electrical resistance R0 is not a constant (it is a linear increasing time series). ΔR is obtained by subtracting a linear trend term from the measured electrical resistance signal. As can be seen in Fig3, the electrical resistance R of all the three types of CNT/cement composites decreases upon loading and increases upon unloading in every cycle under compressive loading, expressing stable and regular piezoresistive responses.

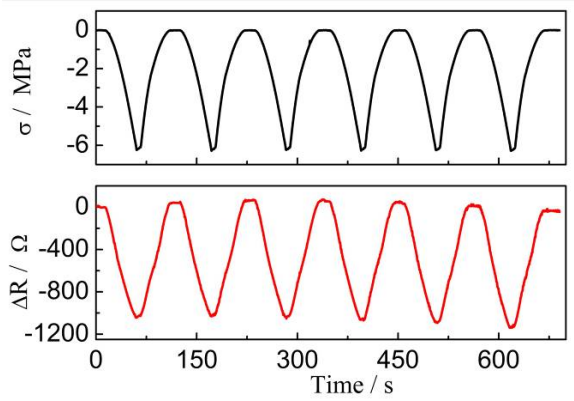

a) With 0.05 wt.% of MWNT (Sample #1)

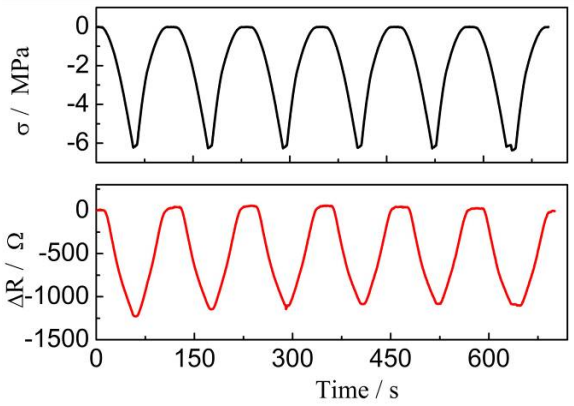

b) With 0.1 wt.% of MWNT (Sample #2)

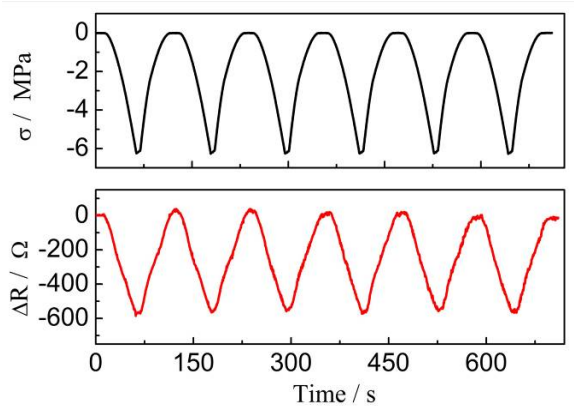

c) With 1 wt.% of MWNT (Sample #3)

Figure 10. Piezoresistivity of CNT/cement composites with different MWNT concentration levels

Figure11 depicts the change amplitudes of the electrical resistance for samples #1, #2 and #3 as the compressive stress is 6MPa. As shown in Figs 11, we find that the change in electrical resistance of samples #1, #2 and #3 reaches about 1000Ω, 1150Ω and 600Ω respectively as compressive stress is 6MPa. This indicates that the CNT/cement composite with 0.1 wt. % of MWNT has the most sensitive response to compressive loading among the three types of CNT/cement composites. It is interesting to note that the composite's piezoresistive sensitivity does not linearly increase with CNT concentration levels. This phenomenon can be explained below. The concentration level of MWNT influences and reflects the situation of network formed in the composites. When the MWNT concentration level is 0.05 wt. %, the thickness of the insulating matrix between adjacent nanotubes is large and the amount of conducted tunneling junction under external loading is low. With the increase of the concentration level of MWNT to 0.1 wt. %, the thickness of the insulating matrix between adjacent nanotubes decreases and the electronic transition by tunneling conduction becomes easy. With the continuous increase of MWNT, the tunneling gap would be further shortened, and then the CNT network stabilizes and becomes hardly to change under loading. This can be proved by SEM photographs as shown in Figure12. Comparing Figure12 b) with Figure12 a), it can be found that the CNT network in CNT/cement composite with 1 wt. % of MWNT is more widespread than that in CNT/cement composite with 0.1 wt. % of MWNT. As a result, the contact resistance of CNT/cement composites with 0.1 wt. % of MWNT is the most sensitive to compressive loading among the fabricated CNT/cement composites. Therefore, the sensitivity of piezoresistive response of CNT/cement composites firstly increases then decreases with the increase of MWNT concentration levels.

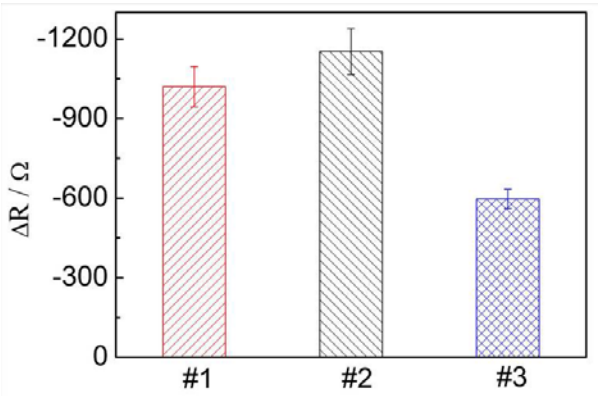

Figure 11. Comparison of electrical resistance changes of CNT/cement composites with different MWNT concentration levels (#1: 0.05 wt. %, #2: 0.1 wt. %, #3: 1 wt. %)

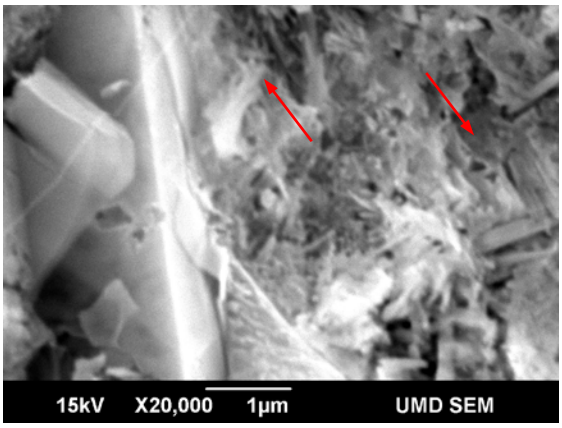

a) With 0.1 wt.% of MWNT (Sample #2)

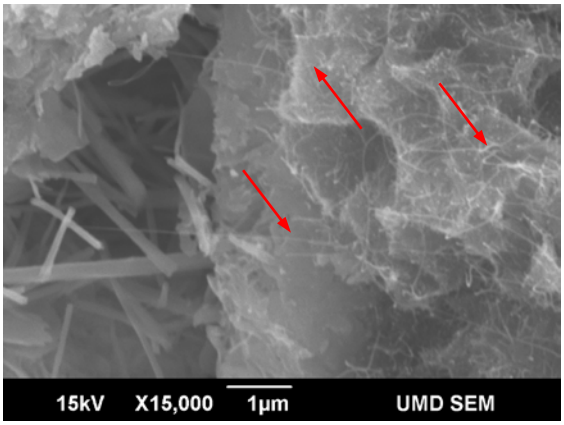

b) With 1 wt.% of MWNT (Sample #3)

Figure 12. SEM photographs of CNT/cement composites

Chapter 4. Road Tests for the Self-Sensing Pavement for Traffic Flow Detection

Road tests for the self-sensing pavement were performed at the outdoor research laboratory of the University of Minnesota Duluth. This facility locates on Interstate highway I-35 southbound, mile point 236, before the exit to Cloquet, Minnesota. Figure13 shows the road test setting. The pavement was cut and the cement-based sensors were embedded into the concrete pavement and fixed with cement paste. Figure 13a) shows the sensors before and after being fixed with cement paste. The sensor array composed of eight sensors is 1.2m in length. The spacing between two adjacent sensors is about 11cm. The sensor array covers half of the lane in width to ensure at least one sensor can be passed over by the vehicle's tire. A car was driven to pass over the sensor array to investigate the feasibility of vehicle detection by using the proposed self-sensing pavement, as shown in Figure 13b).

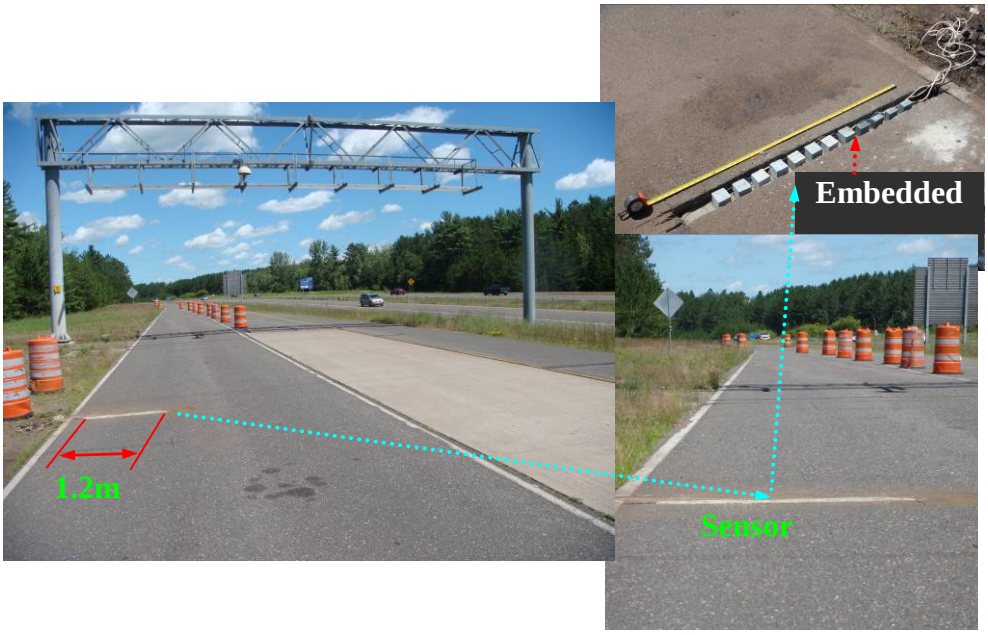

a) Self-sensing pavement embedded with smart cement-based sensor array

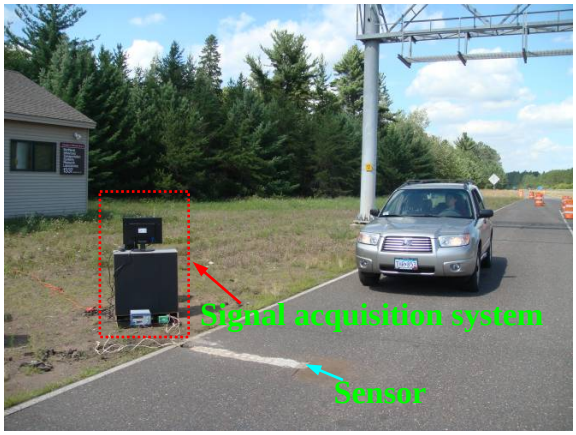

b) Road test

Figure 13. Road test of self-sensing pavement

The sensing property of the smart cement-based sensors is that the electrical resistivity of sensors would change when the sensors subject to external forces. According to Ohm's law, the electrical resistivity ρ_S of the sensors can be expressed as

$$\rho_S = R_S \times \frac{S}{L} \qquad (2)$$

where R_S is electrical resistance of the sensors, S is the sectional area of the sensors and L is the space between two electrodes.

After differential calculation, we can obtain

$$\frac{d\rho_S}{\rho_S} = \frac{dR_S}{R_S} - (1+2\mu)\frac{dL}{L} \tag{3}$$

where μ is Poisson's ratio.

As the deformation of the sensors under compression is very small, the changes in L can be neglected. Correspondingly the change of electrical resistivity can be denoted as

$$\Delta\rho_S / \rho_S = \Delta R_S / R_S \tag{4}$$

It can be seen from Equation (3) that the change in electrical resistivity of the sensors is the same as that in electrical resistance [13, 14].

The circuit diagram of the sensor array and signal acquisition process is depicted in Figure4. As shown this figure, every smart cement-based sensor is series-connected with a constant reference resistance, and so we have

$$\frac{U_{Si}}{R_{Si}} = \frac{U_C - U_{Si}}{R_{Ri}} \tag{5}$$

where R_{Si} and R_{Ri} are the resistance of the ith cement-based sensor and the ith reference resistance respectively. U_{Si} is the voltage at both ends of the ith cement-based sensor. U_C is the external constant voltage of 12V.

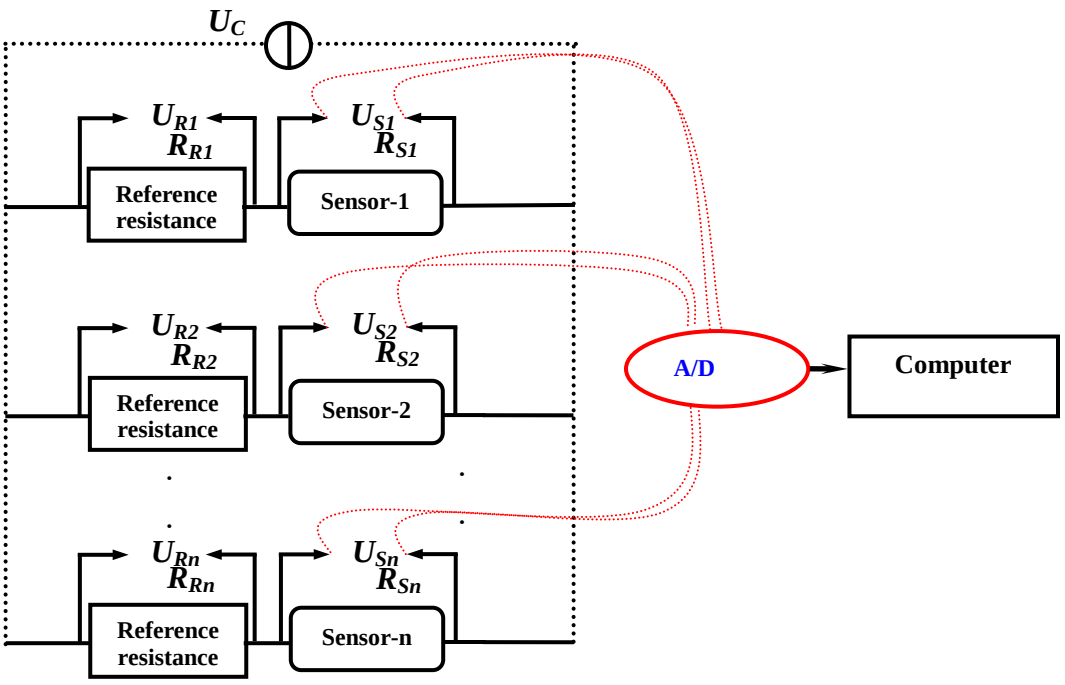

Figure 14. Circuit diagram of sensor array and signal acquisition process

Equation (4) can be further derived as

$$R_{Si} = \frac{U_{Si}}{U_C - U_{Si}} R_{Ri} \qquad (6)$$

If a vehicle is passing over the ith sensor, the resistance of this sensor will vary. The change in resistance of the ith sensor ΔR_{Si} can be expressed as

$$R_{Si} + \Delta R_{Si} = \frac{U_{Si} + \Delta U_{Si}}{U_C - (U_{Si} + \Delta U_{Si})} R_{Ri} \qquad (7)$$

where ΔU_{Si} is the change of the voltage at both ends of the ith sensor.

Since ΔU_{Si} is much smaller than $(U_C - U_{Si})$, Equations (5) and (6) can be combined and derived as

$$\frac{R_{Si} + \Delta R_{Si}}{R_{Si}} = \frac{U_{Si} + \Delta U_{Si}}{U_C - (U_{Si} + \Delta U_{Si})} \times \frac{U_C - U_{Si}}{U_{Si}} \approx \frac{U_{Si} + \Delta U_{Si}}{U_{Si}} \qquad (8)$$

Equation (7) can be further rewritten as

$$\frac{\Delta R_{Si}}{R_{Si}} \approx \frac{\Delta U_{Si}}{U_{Si}} \qquad (9)$$

It can be seen from Equations (3) and (8) that the change in electrical resistivity signal of the sensors caused by vehicular loading is approximately equal to the change in electrical voltage signal. Because voltage signal is more convenient to acquire than electrical resistance signal, the voltage at both ends of the sensors was taken as indices for detecting passing vehicles. As shown in Figure4, an A/D card (PCI-6221 device, National Instruments Corporation, USA) was used to collect the voltage signals of the sensor array. MATLAB and its Real-time Windows Target were used for real-time sampling control. The sampling rate is 500Hz.

Vehicle passing detection tests were performed and the voltage time-histories were collected. The measurement time of each test is about 180s. In order to decrease the effect of measurement noise, a low-pass filter with cut-off frequency of 25Hz was used to pro-process the measured voltage signals. The low-pass filtered and the measured voltage signals are illustrated in Figure 15. As shown in this figure, abrupt changes present in the voltage signal curves when the vehicle passes over the sensor each time. We made a comparison between the measured data and the hand-recorded data, and confirmed that the time points of abrupt changes in the voltage signal curves are consistent with that of the vehicle passing. However, it should be noted that the amplitudes of the signal changes cannot exactly reflect the real vehicle weight, since the tire of the vehicle may partially pass over the sensor. The contact area between the passing vehicle tire and the smart sensors is not equal each detection, so the amplitudes of the abrupt changes in voltage signals are different even for the same car.This could be acceptable for detecting traffic flow rates, vehicular speed and traffic density, since only peak signals are needed to evaluate the three parameters.

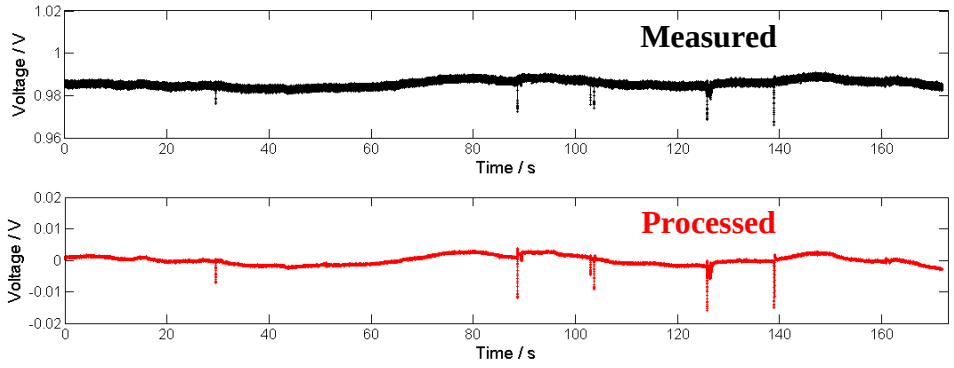

Figure 15. Vehicle passing detection results. Each peak indicates a passing vehicle

Chapter 5. Conclusion and Discussion

Piezoresistive CNT/cement mortars were developed and tested in this study. Experimental results showed that the electrical resistance of the composite changed proportionally to the compressive stress levels. The piezoresistive responses of the composite with different water contend levels and different CNT doping levels were also studied. The CNT based self-sensing pavement shows non-linear responses to water contend levels and CNT doping levels. The composites show promising piezoresitive properties that make them feasible as a stress/strain sensor. The experimental results, including the lab tests and road tests, have demonstrated the potential of using the self-sensing pavement as a traffic flow detector.

References

[1] J. H. Kell, I. J. Fullerton, M. K. Mills, *Traffic Detector Handbook*, U.S. Department of Transportation, Federal Highway Administration, McLean, VA, 1990.

[2] L. A. Klein, *Sensor Technologies and Data Requirements for ITS*, Artech House, Boston, MA, 2001.

[3] Office of Transportation Management, *Freeway Management and Operations Handbook*, U.S. Department of Transportation, Federal Highway Administration, RHWA Report #: FHWA-OP-04-003, McLean, VA, 2003.

[4] S. Iijima, "Helical microtubes of graphitic carbon," *Nature*, vol.354, pp. 56-58, 1991.

[5] M. Meyyappan, edit, *Carbon Nanotubes – Science and applications*, *CRC Press*, New York, NY, 2005.

[6] J. C. Grunlan, A. R. Mehrabi, M. V. Bannon, and J. L. Bahr, "Water-based single-walled-nanotube-filled polymer composite with an exceptionally low percolation threshold," *Advanced Materials*, vol.16, pp. 150-153, 2004.

[7] G. B. Blanchet, S. Subramoney, R. K. Bailey, G. D. Jaycox, and C. Nuckolls, "Sel-assembled three-dimensional conducting network of single-wall carbon nanotubes," *Applied Physics Letters*, vol. 85, pp.828-830, 2004.

[8] Y. J. Kim, T. S. Shin, H. D. Choi, J. H. Kwon, Y.-C. Chung, and H. G. Yoon, "Electrical conductivity of chemically modified multiwalled carbon nanotube/epoxy composites," *Carbon*, vol. 43, pp.23-30, 2005.

[9] T. W. Tombler, C. Zhou, L. Alexseyev, J. Kong, H. Dai, L. Liu, C. S. Jayanthi, M. Tang, and S.-Y. Wu, "Reversible electromechanical characteristics of carbon nanotubes under local-probe manipulation," *Nature*, vol. 405, pp.769-772, 2000.

[10] J. Cao, Q. Wang, and H. Dai, "Electromechanical properties of metallic, quasimetallic, and semiconducting carbon nanotubes under stretching," *Physical Review Letters*, vol. 90, pp.157601-157604, 2003.

[11] R. J. Grow, Q. Wang, J. Cao, D. Wang, and H. Dai, "Piezoresistance of carbon nanotubes on deformable thin-film membranes," *Applied Physics Letters*, vol.86, pp.093104 – 093104-3, 2005.

[12] P. Dharap, Z. Li, S. Nagarajaiah, and E. V. Barrera, "Nanotube film based on single-wall carbon nanotubes for strain sensing," *Nanotechnology*, vol. 15, pp. 379-382, 2004.

[13] I. Kang, M. J. Schulz, J. H. Kim, V. Shanov, and D. Shi, "A carbon nanotube strain sensor for structural health monitoring," *Smart Materials and Structures*, vol. 15, pp.737-748, 2006.

[14] G. Y. Li, P. M. Wang, and X. Zhao, "Mechanical behavior and microstructure of cement composites incorporating surface-treated multi-walled carbon nanotubes," *Carbon*, vol. 43, pp.1239-1245, 2005.

[15] R. L. Jacobsen, T. M. Tritt, J. R. Guth, A. C. Ehrlich, and D. J. Gillespie, "Mechanical properties of vapor-grown carbon fiber," *Carbon*, vol. 33., pp. 1217-1221, 1995.

[16] S. Wen, and D. D. L. Chung, "Piezoresistivity in continuous carbon fiber cement-matrix composite," *Cement and Concrete Research*, vol. 29, pp.445-449, 1999.

[17] S. Wen, S. Wang, and D. D. L. Chung, "Piezoresistivity in continuous carbon fiber polymer-matrix and cement-matrix composite," *Journal of Materials Science*, vol. 35, pp.3669-3675, 2000.

[18] D. D. L. Chung, "Piezoresistive cement-based materials for strain sensing," *Journal of Intelligent Material Systems and Structures*, vol. 13, pp.599-609, 2002.

[19] M. Sun, Q. Liu, Z. Li, and Y. Hu, "A study of piezoelectric properties of carbon fiber reinforced concrete and plain cement paste during dynamic loading," *Cement and Concrete Research*, vol. 30, pp.1593-1595, 2000.

[20] J. Makar, J. Margeson, and J. Luh, "Carbon nanotube/cement composite – early results and potential applications," *3rd International Conference on Construction Materials: Performance, Innovations and Structural Implications*, Vancouver, B. C., pp. 1-10, Aug. 22-24, 2005.